Improved a-$B_{10}C_{2+x}H_y$/Si p-n heterojunction performance after neutron irradiation

George Glenn Peterson, Qing Su, Yongqiang Wang, Natale J. Ianno, Peter A. Dowben, and Michael Nastasi

Citation: Journal of Vacuum Science & Technology B **36**, 011207 (2018); doi: 10.1116/1.5008999
View online: https://doi.org/10.1116/1.5008999
View Table of Contents: http://avs.scitation.org/toc/jvb/36/1
Published by the American Vacuum Society

Articles you may be interested in

Characterization of photoresist films exposed to high-dose implantation conditions
Journal of Vacuum Science & Technology B, Nanotechnology and Microelectronics: Materials, Processing, Measurement, and Phenomena **36**, 011201 (2018); 10.1116/1.5004127

10 MeV proton damage in β-Ga_2O_3 Schottky rectifiers
Journal of Vacuum Science & Technology B **36**, 011206 (2018); 10.1116/1.5013155

Numerical and experimental thermal analysis of polyimide-based x-ray masks at the Canadian Light Source
Journal of Vacuum Science & Technology B, Nanotechnology and Microelectronics: Materials, Processing, Measurement, and Phenomena **36**, 012001 (2018); 10.1116/1.5005115

Frequency dispersion and dielectric relaxation in postdeposition annealed high-κ erbium oxide metal–oxide–semiconductor capacitors
Journal of Vacuum Science & Technology B, Nanotechnology and Microelectronics: Materials, Processing, Measurement, and Phenomena **36**, 012201 (2018); 10.1116/1.4995809

Low temperature bonding of heterogeneous materials using Al_2O_3 as an intermediate layer
Journal of Vacuum Science & Technology B, Nanotechnology and Microelectronics: Materials, Processing, Measurement, and Phenomena **36**, 011202 (2018); 10.1116/1.5005591

Extreme-low k porous pSiCOH dielectrics prepared by PECVD
Journal of Vacuum Science & Technology B, Nanotechnology and Microelectronics: Materials, Processing, Measurement, and Phenomena **36**, 012202 (2018); 10.1116/1.5007177

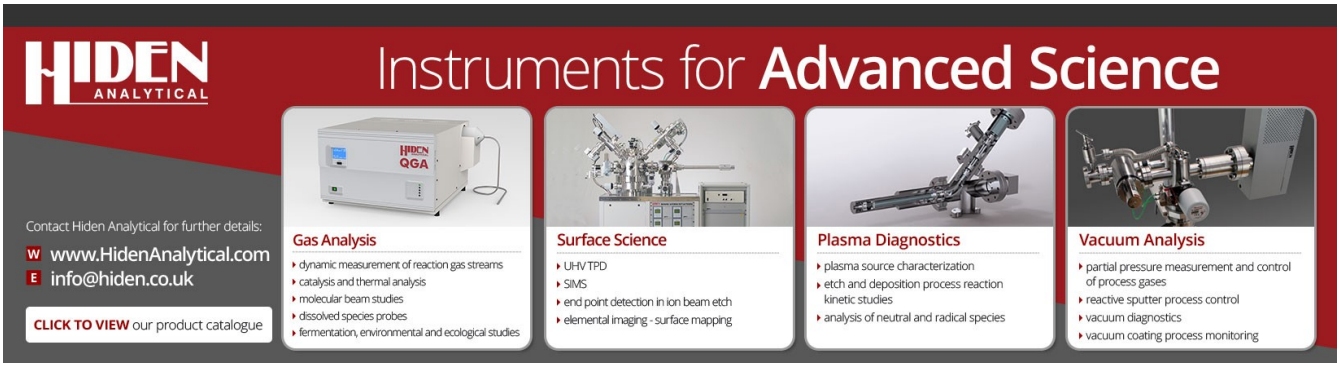

Improved a-$B_{10}C_{2+x}H_y$/Si p-n heterojunction performance after neutron irradiation

George Glenn Peterson
Department of Mechanical and Materials Engineering, University of Nebraska, W342 NH, Lincoln, Nebraska 68588-0526

Qing Su
Nebraska Center for Energy Sciences Research, University of Nebraska, 230 Prem S. Paul Research Center at Whittier School, 2200 Vine Street, Lincoln, Nebraska 68583-0857

Yongqiang Wang
Materials Science and Technology Division, Los Alamos National Laboratory, Los Alamos, New Mexico 87545

Natale J. Ianno
Department of Electrical and Computer Engineering, University of Nebraska, 209N Scott Engineering Center, P.O. Box 880511, Lincoln, Nebraska 68588-0511

Peter A. Dowben
Department of Physics and Astronomy, University of Nebraska, 208 Theodore Jorgensen Hall, 855 N 16th Street, Lincoln, Nebraska 68588-0299

Michael Nastasi[a)]
Nebraska Center for Energy Sciences Research, University of Nebraska, 230 Prem S. Paul Research Center at Whittier School, 2200 Vine Street, Lincoln, Nebraska 68583-0857

(Received 11 October 2017; accepted 12 December 2017; published 12 January 2018)

The impact of neutron irradiation, in the energy range of ~0.025 eV, on amorphous semiconducting partially dehydrogenated boron carbide (a-$B_{10}C_{2+x}H_y$) on silicon p-n heterojunction diodes was investigated. The heterojunction devices were created by synthesizing a-$B_{10}C_{2+x}H_y$ via plasma enhanced chemical vapor deposition on n-type silicon. Unlike many electronic devices, the performance of the a-$B_{10}C_{2+x}H_y$ heterojunction diode improved with neutron irradiation, in spite of the large neutron cross section of ^{10}B. There is also increased charge carrier lifetime of more than 200% with modest neutron irradiation of approximately 2.7×10^8 to 1.08×10^9 neutrons/cm^2. *Published by the AVS.* https://doi.org/10.1116/1.5008999

I. INTRODUCTION

Boron rich semiconducting icosahedral based materials have been investigated for application in solid-state neutron detection[1–12] and as a potential neutron voltaic[13,14] for some time.[15] While there have been numerous studies of the structural changes in boron carbides as a result of irradiation,[16–30] most studies involve hot-pressed/sintered or sputtered samples, rather than plasma enhanced chemical vapor deposition (PECVD) samples. The distinction being that PECVD synthesized boron carbide films may retain some fraction of their source molecule hydrogen,[31–34] and are not very likely to be exceedingly crystalline. Of the studies that do focus on PECVD synthesized boron carbide, very few studies have focused on the changes in electrical characteristics as a result of irradiation. Those studies, however, suggest that the icosahedral boron carbide[31,35] and boron phosphide[28,29] based devices improve with some He^+ ion irradiation exposure, and are robust against radiation induced device degradation and failure. These results indicate but do not conclusively show that such devices are robust against neutron irradiation that results in neutron capture by ^{10}B and then fragmentation into energetic $^7Li/^4He^{++}$ ion pairs.

Prior studies indicated that the heterojunction boron carbide device failure, under He^+ ion irradiation, is the result of damage in the crystalline silicon (c-Si) substrate,[31] not the boron carbide. It was suggested[31] that the damage to the silicon was mostly due to elastic collisions of the incident ion with the c-Si atoms near the ion end of range where Frenkel pairs, ion implantation, and extended defects form, although other mechanisms have also been put forward.[23,36,37] Here is an effort to provide additional insight into the changes of the device as a result of neutron irradiation induced changes in the amorphous partially dehydrogenated semiconducting boron carbide film, as well as to conclusively show that such devices are robust against neutron irradiation.

II. EXPERIMENT

Device synthesis begins with an n-type silicon (P doped) substrate (001) of resistivity 65–110 Ω cm (University Wafers). The silicon substrates were cleaned in sequential sonication baths of acetone, methanol, and filtered deionized water followed by a 5 wt. % hydrofluoric acid bath for oxide removal and hydrogen termination.[38] Prior to deposition, the substrate was exposed to a 30 min Ar^+ plasma etch to remove any residual carbon or other surface impurities. The amorphous semiconducting partially dehydrogenated boron

[a)]Electronic mail: mnastasi2@unl.edu

carbide thin films were synthesized via PECVD utilizing orthocarborane (*closo*-1,2 dicarbadodecaborane, $C_2B_{10}H_{12}$) (Sigma Aldrich) as the source compound for the hydrogenated semiconducting boron carbide and argon to raise the background pressure to make the plasma sustainable. Details of the deposition process have been previously reported.[2–5,8–14,31,39] The reported stoichiometric compositions of semiconducting amorphous partially dehydrogenated boron carbide films vary widely.[40,41] This is represented as *a*-$B_{10}C_{2+x}H_y$ with $0 < x < 3$ and $0 < y < 12$. For this study, as established by elastic recoil detection measurements,[31] x is approximately 0 and y is approximately 4.

To fabricate functional devices, Cr contact metallization, with an Au capping layer, was deposited through a dc magnetron sputter source (AJA International, Inc.) at a base pressure below 1×10^{-7} Torr. Both metals were sputtered with an Ar^+ plasma at a pressure of 5 mTorr to a thickness of approximately 300 nm.

A deuterium-tritium (D-T) neutron source (Thermo Scientific MP 320 neutron generator) was utilized for neutron irradiation. This D-T source produces 14 MeV neutrons, and was combined with a 10 cm beryllium (Be) cube neutron multiplier. These neutrons were moderated by 1 in. of paraffin, providing approximately 7500 neutrons/cm^2 s with a slightly anisotropic 4π neutron environment for the irradiated samples (opposed to a directional irradiation beam emanating from the generator). Flux calibration, neutron moderation, and generator to sample geometry is outlined elsewhere.[39]

Capacitance versus voltage measurements were obtained using an HP model 4192A impedance analyzer with an oscillation voltage set to 0.010 v in a four-point parallel circuit, detailed previously.[35]

III. RESULTS

Creation of ^{7}Li (0.84 MeV) and α ($^4He^{++}$) (1.47 MeV), the fragments (ions), following neutron capture by a ^{10}B atom, leads to the production of an excess of 10^6 electron–hole pairs. From *Monte Carlo* stopping and range of ions in matter (SRIM) code simulations,[42] the ^{7}Li ion has a range of approximately 2.5 μm, and the α has a range of approximately 5.2 μm in Si. Upon fragmentation and translation away from the capture site, the direction of translation is completely random with equal chances of translating into the Si substrate, out of the top of the film, parallel to the interface plane, and all angles in between (with the ^{7}Li and α translating in opposite directions), as shown in Fig. 1.

There are two types of energy deposition from an irradiating ion: electronic stopping (ionization energy) and elastic collisions (recoil energy).[43] Ionization energy deposition represents a sudden perturbation to the system by the transfer of energy from the irradiating ion to the electrons of the target atoms. This results in the breaking of bonds, if the energy deposition rate per atom is larger than the bonding energy. Recoil energy deposition is due to collisions between the irradiating ion and the target atom nuclei, causing cascades of displacement damage in the form of Frenkel pairs and

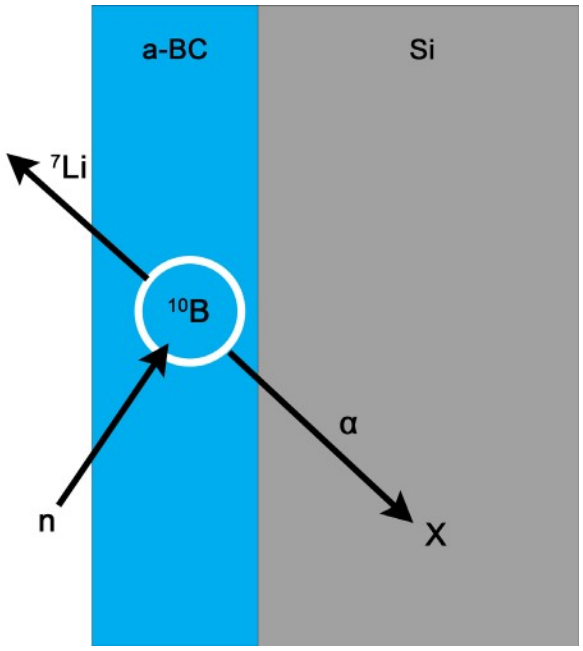

FIG. 1. (Color online) Depiction of neutron capture by a ^{10}B isotope resulting in fragmentation into a ^{7}Li and α particle pair with kinetic energy resulting in translation away from the capture site (not to scale). Unless ion translation is parallel to the interface, one ion will exit the *a*-$B_{10}C_{2+x}H_y$ film, and one will implant within the Si substrate, as represented by the "**x**."

extended defects. The transmission electron microscopy and SRIM analysis, as reported elsewhere,[31] showed that initial energy deposition by an incident ion (200 keV He^+) will be dominated by ionization energy. Only with sufficient kinetic energy loss (in penetration range or depth where ion implantation occurs) will the α energy loss occur predominantly through recoil energy deposition. The unirradiated (virgin) film thickness is approximately 192 nm (as indicated by ellipsometric measurement: J.A. Woollam Company M-2000VI). As stated earlier, the daughter fragments after neutron capture by a ^{10}B atom, ^{7}Li and $^4He^+$ ions, have an effective range of 2.5 and 5.2 μm in Si, respectively. The rate of ionization energy deposition is very similar in both the Si substrate and *a*-$B_{10}C_{2+x}H_y$ film, meaning that the ion range or path length in the *a*-$B_{10}C_{2+x}H_y$ film will be of a similar magnitude (i.e., larger than 1 μm). This means that only if the translational direction is parallel to the interface plane will the ^{7}Li or α particles terminate inside of the *a*-$B_{10}C_{2+x}H_y$ film, and allows for the assumption that the vast majority of energy deposition within the *a*-$B_{10}C_{2+x}H_y$ film is ionization energy—bond breaking as opposed to displacement damage due to elastic collisions.

From the diode $I(V)$ curves of Fig. 2, for an *a*-$B_{10}C_{2+x}H_y$/*Si* heterojunction diode after 0, 2.7×10^8, 5.4×10^8, and 10.8×10^8 neutrons/cm^2 exposure (0, 10, 20, and 40 h of exposure to neutron irradiation, under our experimental conditions), it is evident that the $I(V)$ curve shows that the device performance improves with small amounts of neutron irradiation, notably to 2.7×10^8 neutrons/cm^2 exposure. Evidence of diode improvement is taken from both the increase in magnitude of forward bias current as well as a

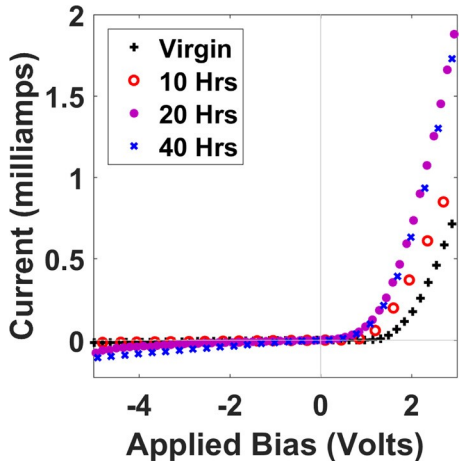

FIG. 2. (Color online) Current vs voltage curves of a *a*-$B_{10}C_{2+x}H_y$ to silicon heterojunction diode following 0, 2.7×10^8, 5.4×10^8, and 10.8×10^8 neutrons/cm^2 exposure (0, 10, 20, and 40 h of exposure to neutron irradiation, under our experimental conditions).

decrease in the turn-on voltage. For the following discussion, the turn-on voltage was determined by extrapolating a linear fit of the data in the large forward bias region [i.e., 2 to 1 V for the 10.8×10^8 neutrons/cm^2 (40 h) irradiated sample] to a diode current of zero. In comparing the diode current in Fig. 2, the value at 1.55 V was chosen because that applied bias is slightly greater than the highest turn-on voltage. In the forward bias region, it is immediately evident that after 10 h of irradiation (○) corresponding to roughly 2.7×10^8 neutrons/cm^2, the diode current increases by 325.9%, and the device turn-on voltage decreases from 1.52 to 1.25 V. After 20 h of irradiation (●), the diode current is more than seven times (roughly 686%) greater than the unirradiated (+) device, and the turn-on voltage is 1.16 V, a decrease of 23.7% from the unirradiated device. After 40 h of irradiation (×), corresponding to roughly 10.8×10^8 neutrons/cm^2, the diode current is still more than seven times (roughly 618%) greater than the unirradiated device, and the turn on voltage remains 1.16 V.

In the reverse bias region of the $I(V)$ curves, after 10 h of irradiation, there is a decrease in the reverse bias current (i.e., increased current rectification) of 13.2% at an applied bias of −10 V. After 20 h of irradiation, this trend reverses, and the reverse bias current has increased more than four times (roughly 388%) at an applied bias of −5 V over the virgin reverse bias current. After 40 h of irradiation, the reverse bias current has increased by more than seven times (roughly 605%) over the virgin reverse bias current at an applied bias of −5 V. Of key importance is the increase in forward bias current and the decrease in reverse bias current that occurs with these boron carbide heterojunction at 2.7×10^8 neutrons/cm^2 exposure (10 h of exposure to neutron irradiation, under our experimental conditions). The devices improve, not degrade, with this 2.7×10^8 neutrons/cm^2 exposure to epithermal neutrons, by this $I(V)$ curve measurement. There are other indicators that these boron carbide heterojunction devices improve, rather than degrade, with exposure to epithermal neutrons.

As established in our previous works,[32,44] to examine charge carrier lifetime we also require capacitance vs voltage measurements as shown in Fig. 3. The capacitance associated with oscillations in the depletion width due to small sinusoidal perturbations is referred to as the junction capacitance (C_J). In the case of a heterojunction, C_J is described by[45]

$$C_J = \left(\frac{qN_1N_2\varepsilon_1\varepsilon_2\varepsilon_0}{2(\varepsilon_1N_1 + \varepsilon_2N_2)(\varphi_{bi} - V_A)} \right)^{\frac{1}{2}}, \quad (1)$$

where q is the elemental charge, ε_0 is the permittivity of free space, N_1 is the number of donor atoms/m^3 in the n-type material, N_2 is the number of acceptor atoms/m^3 in the p-type material, ε_1 is the dielectric constant of the n-type material, ε_2 is the dielectric constant of the p-type material, φ_{bi} is the device built-in voltage, and V_A is the applied voltage. If there are no other charge oscillations, the device capacitance, independent of frequency, is equal to C_J in reverse bias (depletion conditions).[46] Figure 3 plots the capacitance versus voltage $C(V)$ curves, taken at 100 kHz. for a *a*-$B_{10}C_{2+x}H_y$/Si p-n heterojunction device after 0, 2.7×10^8, 5.4×10^8, and 10.8×10^8 neutrons/cm^2 exposure (0, 10, 20, and 40 h of exposure to neutron irradiation, under our experimental conditions). Although not shown here, the reverse bias capacitance for all irradiation exposure times and frequencies of 10, 100, and 1000 kHz all remain between 0.17 and 0.38 nF [i.e., the $C(V)$ is very frequency independent].

In reverse bias, the device capacitance is dominated by the junction capacitance, even after 40 h of neutron irradiation (estimated fluence 10.8×10^8 neutrons/cm^2). The frequency independence of the junction capacitance indicates that simple parallel plate model of capacitance in reverse bias is reasonable in this frequency range.

Due to the sinusoidal perturbation signal in forward bias, there is a significant contribution by the minority carriers to the changes in charge concentration. This contribution to the device capacitance is referred to as the diode diffusion capacitance (C_D), and is given by the following equation:[47]

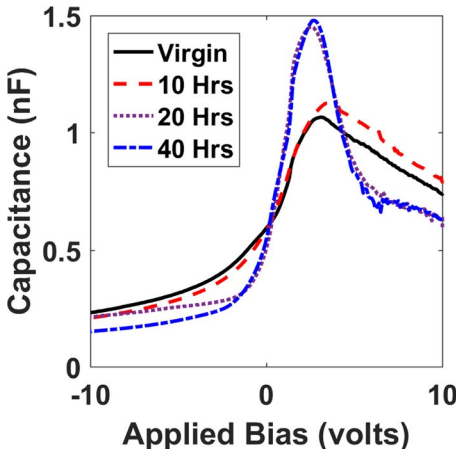

FIG. 3. (Color online) Capacitance vs voltage $C(V)$ curves taken at 100 kHz of *a*-$B_{10}C_{2+x}H_y$/Si p-n heterojunction device after 0, 2.7×10^8, 5.4×10^8, and 10.8×10^8 neutrons/cm^2 exposure (0, 10, 20, and 40 h of exposure to neutron irradiation, under our experimental conditions).

$$C_D = \frac{G_0}{\omega\sqrt{2}}\left(\sqrt{1+\omega^2\tau^2}-1\right)^{\frac{1}{2}}, \quad (2)$$

where G_0 is the low frequency conductance (forward bias), ω is the angular frequency $(2\pi f)$, and τ is the effective carrier lifetime (as shown in Fig. 4). There are many and various contributions to the capacitances, and many types of defects, but if we restrict our modeling efforts to the diffusion component of transport, Eq. (2) can be used to model the data relative to the baseline capacitance of Fig. 3.

The technique for calculating the charge carrier lifetime for boron carbide heterojunction diodes has been discussed extensively.[32,44] This lifetime technique has been performed for 0 (or no neutrons above background), 2.7×10^8, 5.4×10^8, and 10.8×10^8 neutrons/cm^2 exposure (0, 10, 20, and 40 h of exposure to neutron irradiation, under our experimental conditions). The results are shown in Fig. 4 as the right hand vertical axis (dashed line). The indicated charge carrier lifetime for the unirradiated sample is 0.95 μs, after 10 h of irradiation this increases to 1.20 μs, after 20 h of irradiation this is further increased to 3.00 μs, and after 40 h of irradiation this trend reverses and is decreased to 1.30 μs.

A. Discussion

The p-n junction device current versus voltage $I(V)$ curves shown in Fig. 2 were used to establish one "Figure of Merit" for device performance. A second figure of merit is shown in Fig. 4 (left axis). This figure of merit (previously used in the characterization of device degradation under He^+ ion irradiation[31]) is the ratio of the differential diode conductance, a ratio of the low frequency diode conductance ($G_0 = dI/dV$) under forward bias to the low frequency diode conductance under reverse bias. G_0 for both forward and reverse bias conditions were extracted from the $I(V)$ data in the range 0.75 to 1.00 applied volts. The higher the ratio, the better the heterojunction diode performance (figure of merit), as in previous works.[31,32,44,48] This is plotted in Fig. 4 with the error bars representing the standard deviation for the voltage range. After 2.7×10^8 neutrons/cm^2 exposure (10 h of irradiation), the increase in device current and slight increase in current rectification results in a better performing device with an increase in the ratio from 0.8 to 26.4. After 5.4×10^8 neutrons/cm^2 exposure (20 h of irradiation), the significant increase in forward bias diode current causes the G_0 ratio to increase to 47.4. After 10.8×10^8 neutrons/cm^2 exposure (40 h of irradiation), the G_0 ratio has decreased to 9.1, representing the onset of device degradation (i.e., current rectification decreases). The differential diode conductance figure of merit (Fig. 4), G_0, shows that the change in device performance with neutron irradiation has a very similar response to that of He^+ ion irradiation reported in a previous work.[31] Figure 4 also shows that there may be a correlation between the charge carrier lifetime, effectively a second figure of merit, and diode performance.

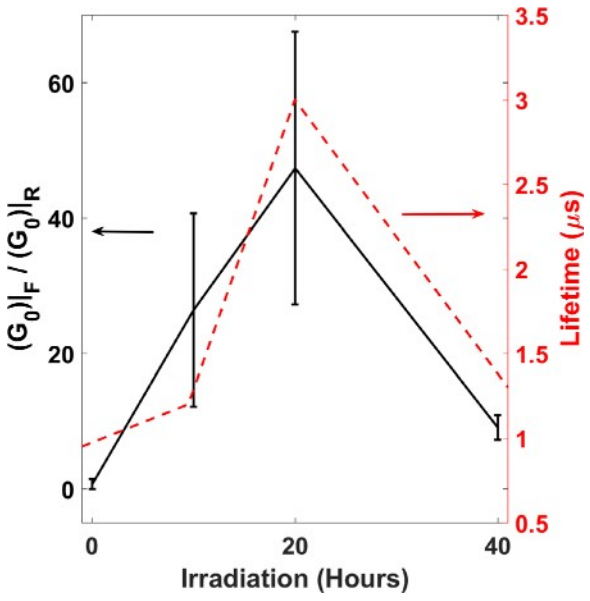

FIG. 4. (Color online) (Left axis) Ratio of the derivative of forward bias current with respect to voltage by the derivative of reverse bias current with respect to voltage derived from $I(V)$ data taken between 0.75 and 1.00 applied volts. The higher the ratio, the better the heterojunction diode performance (figure of merit). (Right axis) The effective carrier lifetime as a function of neutron irradiation, i.e., 0, 2.7×10^8, 5.4×10^8, and 10.8×10^8 neutrons/cm^2 exposure (0, 10, 20, and 40 h of exposure to neutron irradiation, under our experimental conditions), as indicated by C_D modeling.

Thermal neutron irradiation of the crystalline silicon (c-Si) has a significant atomic cross-section for scattering events, but not for capture or displacement events ($m_{neutron} \ll m_{Si}$). As a result, the c-Si lattice structure should only be perturbed by the energetic ^{7}Li (0.84 MeV) and α ($^4He^{++}$) (1.47 MeV) pairs created by ^{10}B neutron capture events, in the boron carbide layer of the heterojunction. The neutron fluence and capture probability (as outlined in Sec. II) should be such that the damage within the c-Si substrate is minimal, in this experiment. We anticipate that for this experiment, any changes in electrical or structural characteristics should be isolated to the amorphous partially dehydrogenated semiconducting boron carbide film, not due to the large amounts of damage in the c-Si substrate observed previously.

In an effort to identify changes in the device as a function of irradiation, high resolution transmission electron microscopy (HRTEM) images and selected area electron diffraction patterns were obtained both of the *a*-$B_{10}C_{2+x}H_y$/Si interface, and in the bulk Si far from the interface (800 nm), but still within the ^{7}Li and α particle range (not shown here). No discernable damage could be detected in either the *a*-$B_{10}C_{2+x}H_y$ or the Si substrate, in either HTREM image or the SAED pattern; however, point defects in Si are undetectable with this technique until they occur in concentrations high enough that point defect agglomeration begins to occur.[31] This is in agreement with previous findings that device improvement, as a result of irradiation, is not due to changes in the interface, changes in the structure of the amorphous material, or changes in the structure of the crystalline material.[31] Instead, these findings support our previous supposition that the device improvement is due to defect passivation of the amorphous material as a result of the ionization energy deposition from the ^{7}Li/α particle pairs.

IV. SUMMARY AND CONCLUSIONS

In conclusion, amorphous partially dehydrogenated semiconducting boron carbide was synthesized via PECVD on n-type single crystal silicon. This research provides evidence that the electrical properties of amorphous partially dehydrogenated semiconducting boron carbide on silicon p-n heterojunction diodes initially improve with neutron irradiation, contrary to nearly all traditional electronic devices. The cause for the device improvement is most likely a result of defect passivation within the *a*-$B_{10}C_{2+x}H_y$ film.

This research indicates that some disorder within the amorphous semiconductor film (in the form of defects) allows for healing with initial irradiation. This increases the operational lifetime of the device. Further, if defect passivation is the driving force behind device improvement, this may change the carrier concentration of the *a*-$B_{10}C_{2+x}H_y$ film (toward a more intrinsic material) if some of the passivated defects had contributed to the carrier concentration. Such changes should be evident in the built-in potential of each constituent semiconducting material comprising the heterojunction structure. The device built-in potential (φ_{bi}) is the sum of the built-in potential within each constituent semiconducting material (i.e., the narrow band-gap material and the wide band-gap material). Future research efforts will focus on attempting to directly measure, model, or deduce changes in the built-in potential to provide concrete evidence explaining the results reported here.

ACKNOWLEDGMENTS

This work was supported by the Office of Research and Economic Development at the University of Nebraska–Lincoln, the Defense Threat Reduction Agency (Grant No. HDTRA1-14-1-0041), and the Office of Naval Research (Contract Nos. FA4600-12-D-9000-0045 and FA4600-12-D-9000-0057). This work was performed, in part, at the Center for Integrated Nanotechnologies, an Office of Science User Facility operated for the U.S. Department of Energy (DOE) Office of Science. Los Alamos National Laboratory, an affirmative action equal opportunity employer, is operated by Los Alamos National Security, LLC, for the National Nuclear Security Administration of the U.S. Department of Energy under Contract No. DE-AC52-06NA25396. The work was carried out in part in the Central Facilities of the Nebraska Center for Materials and Nanoscience, which is supported by the Nebraska Research Initiative. The authors would like to acknowledge S. Ducharme of the Department of Physics and Astronomy at the University of Nebraska–Lincoln for allowing the use of his laboratory's impedance analyzer. The authors would like to acknowledge S. Adenwalla of the Department of Physics and Astronomy at the University of Nebraska–Lincoln for allowing the use of her laboratory's neutron generator which was funded in part by the Office of Research and Economic Development (ORED).

[1]A. N. Caruso, J. Phys. Condens. Matter **22**, 443201 (2010).
[2]A. N. Caruso, R. B. Billa, S. Balaz, J. I. Brand, and P. A. Dowben, J. Phys. Condens. Matter **16**, L139 (2004).
[3]B. W. Robertson, S. Adenwalla, A. Harken, P. Welsch, J. I. Brand, P. Dowben, and J. P. Claassen, Appl. Phys. Lett. **80**, 3644 (2002).
[4]S. Adenwalla, R. Billa, J. I. Brand, E. Day, M. J. Diaz, A. Harken, A. McMullen-Gunn, R. Padmanabhan, and B. W. Robertson, Proc. SPIE **5199**, 70 (2004).
[5]B. W. Robertson, S. Adenwalla, A. Harken, P. Welsch, J. I. Brand, J. P. Claassen, N. M. Boag, and P. A. Dowben, Proc. SPIE **4785**, 226 (2002).
[6]K. Osberg, N. Schemm, S. Balkir, J. I. Brand, S. Hallbeck, and P. Dowben, "A hand-held neutron detection sensor system," *2006 IEEE International Symposium on Circuits and Systems (ISCAS 2006) Proceedings* (2006) pp. 1179–1182.
[7]K. Osberg, N. Schemm, S. Balkir, J. I. Brand, M. S. Hallbeck, P. A. Dowben, and M. W. Hoffman, IEEE Sens. J. **6**, 1531 (2006).
[8]A. N. Caruso *et al.*, Mater. Sci. Eng. B **135**, 129 (2006).
[9]E. Day, M. J. Diaz, and S. Adenwalla, J. Phys. Appl. Phys. **39**, 2920 (2006).
[10]N. Hong, J. Mullins, K. Foreman, and S. Adenwalla, J. Phys. Appl. Phys. **43**, 275101 (2010).
[11]N. Hong, L. Crow, and S. Adenwalla, Nucl. Instrum. Methods Phys. Res., Sect. A **708**, 19 (2013).
[12]E. Echeverría *et al.*, Appl. Phys. A **118**, 113 (2014).
[13]R. Bao, Z. Yan, and D. B. Chrisey, Appl. Phys. Lett. **98**, 192106 (2011).
[14]E. Echeverría, R. James, F. L. Pasquale, J. A. Colón Santana, M. S. Driver, A. Enders, J. A. Kelber, and P. A. Dowben, in *Symposium on DD/WW–Materials and Radiation Effects for Advanced Nuclear Technologies* (2015).
[15]H. E. Robson, "Vapor pressure and thermodynamic properties of boron carbide," Ph.D. thesis (University of Kansas, 1959).
[16]T. Maruyama, M. Iwanami, S. Ohnuki, T. Suda, S. Watanabe, and K. Ikezawa, in *21st International Symposium on Effects of Radiation on Materials*, edited by M. Grossbeck, T. Allen, R. Lott, and A. Kumar (ASTM International, West Conshohocken, PA, 2004), pp. 670–680.
[17]C. Höglund, K. Zeitelhack, P. Kudejova, J. Jensen, G. Greczynski, J. Lu, L. Hultman, J. Birch, and R. Hall-Wilton, Radiat. Phys. Chem. **113**, 14 (2015).
[18]A. Aitkaliyeva, M. C. McCarthy, H.-K. Jeong, and L. Shao, Nucl. Instrum. Methods Phys. Res. Sect. B **272**, 249 (2012).
[19]M. W. Mortensen, P. G. Sørensen, O. Björkdahl, M. R. Jensen, H. J. G. Gundersen, and T. Bjørnholm, Appl. Radiat. Isot. **64**, 315 (2006).
[20]G. Victor *et al.*, Nucl. Instrum. Methods Phys. Res. Sect. B **365**, 30 (2015).
[21]G. Nowak *et al.*, J. Appl. Phys. **117**, 34901 (2015).
[22]B. Todorović-Marković, I. Draganić, D. Vasiljević-Radović, N. Romčević, M. Romčević, M. Dramićanin, and Z. Marković, Appl. Surf. Sci. **253**, 4029 (2007).
[23]D. Simeone, C. Mallet, P. Dubuisson, G. Baldinozzi, C. Gervais, and J. Maquet, J. Nucl. Mater. **277**, 1 (2000).
[24]K. J. Riley, P. J. Binns, S. J. Ali, and O. K. Harling, Phys. Med. Biol. **49**, 2015 (2004).
[25]M. W. Mortensen, O. Björkdahl, P. G. Sørensen, T. Hansen, M. R. Jensen, H. J. G. Gundersen, and T. Bjørnholm, Bioconjugate Chem. **17**, 284 (2006).
[26]R. G. Abrefah, R. B. M. Sogbadji, E. Ampomah-Amoako, S. A. Birikorang, H. C. Odoi, and B. J. B. Nyarko, Appl. Radiat. Isot. **69**, 85 (2011).
[27]J. Ghassoun and N. Senhou, Appl. Radiat. Isot. **70**, 620 (2012).
[28]M. Carrard, D. Emin, and L. Zuppiroli, Phys. Rev. B **51**, 11270 (1995).
[29]D. Emin, J. Solid State Chem. **179**, 2791 (2006).
[30]M. McPherson, T. Sloan, and B. K. Jones, J. Phys. Appl. Phys. **30**, 3028 (1997).
[31]G. Peterson, Q. Su, Y. Wang, P. A. Dowben, and M. Nastasi, Mater. Sci. Eng. B **202**, 25 (2015).
[32]E. Echeverria *et al.*, J. Phys. Appl. Phys. **49**, 355302 (2016).
[33]M. S. Driver, M. M. Paquette, S. Karki, B. J. Nordell, and A. N. Caruso, J. Phys. Condens. Matter **24**, 445001 (2012).
[34]B. J. Nordell *et al.*, J. Appl. Phys. **118**, 35703 (2015).
[35]G. G. Peterson, Y. Wang, N. J. Ianno, and M. Nastasi, IEEE Trans. Nucl. Sci. **63**, 2815 (2016).
[36]J. E. Bevins, K. R. Dahl, J. W. McClory, J. C. Petrosky, and A. N. Caruso, J. Radiat. Eff. Res. Eng. **30**, 33 (2012).
[37]T. Stoto, N. Housseau, L. Zuppiroli, and B. Kryger, J. Appl. Phys. **68**, 3198 (1990).

[38]G. W. Trucks, K. Raghavachari, G. S. Higashi, and Y. J. Chabal, Phys. Rev. Lett. **65**, 504 (1990).
[39]N. Hong, *An Exploration of Neutron Detection in Semiconducting Boron Carbide* (University of Nebraska, Lincoln, 2012).
[40]C. Pallier *et al.*, Chem. Mater. **25**, 2618 (2013).
[41]S. Lee, J. Mazurowski, G. Ramseyer, and P. A. Dowben, J. Appl. Phys. **72**, 4925 (1992).
[42]J. P. Biersack and L. G. Haggmark, Nucl. Instrum. Methods **174**, 257 (1980).
[43]M. Nastasi and J. W. Mayer, *Ion Implantation and Synthesis of Materials* (Springer, Berlin Heidelberg, 2006).
[44]D. A. Oulianov, R. A. Crowell, D. J. Gosztola, I. A. Shkrob, O. J. Korovyanko, and R. C. Rey-de-Castro, J. Appl. Phys. **101**, 053102 (2007).
[45]A. J. Elliot, "Rate constants and G-values for the simulation of the radiolysis of light water over the range 0-300C," AECL Report No. 11073, Chalk River Laboratories, Chalk River, ON, Canada, 1994.
[46]Y. Tabata, I. Itoh, and S. Tagawa, *CRC Handbook of Radiation Chemistry* (CRC, Boca Raton, 1991).
[47]Y. Young, *Physics in Today's World*, edited by A. Newman (Springer, New York, 1999), Vol. 2, pp. 62–68.
[48]J. Nelson, U.S. patent 5,693,000 (12 December 2005).